

Influence of an inserted bar on the flow regimes in the hopper

Yi Peng(彭毅), Sheng Zhang(张晟), Mengke Wang(王梦柯), Guanghui Yang(杨光辉), Jiangfeng Wan(万江锋), Liangwen Chen(陈良文), and Lei Yang(杨磊)

Citation: Chin. Phys. B, 2021, 30 (**2**): 028101. DOI: 10.1088/1674-1056/abcf40
Journal homepage: http://cpb.iphy.ac.cn; http://iopscience.iop.org/cpb

What follows is a list of articles you may be interested in

Morphological modifications of C_{60} crystal rods under hydrothermal conditions

Ming-Run Du(杜明润), Shi-Xin Liu(刘士鑫), Jia-Jun Dong(董家君), Ze-Peng Li(李泽朋), Ming-Chao Wang (王明超), Tong Wei(魏通), Qing-Jun Zhou(周青军), Xiong Yang(杨雄), and Peng-fei Shen(申鹏飞)
Chin. Phys. B, 2020, 29 (**12**): 128102. DOI: 10.1088/1674-1056/abc0d8

Theoretical studies on alloying of germanene supported on Al (111) substrate

Qian-Xing Chen(陈前行), Hao Yang(杨浩), and Gang Chen(陈刚)†
Chin. Phys. B, 2020, 29 (**10**): 108103. DOI: 10.1088/1674-1056/ab9c08

A numerical study of dynamics in thin hopper flow and granular jet

Meng-Ke Wang(王梦柯), Guang-Hui Yang(杨光辉), Sheng Zhang(张晟), Han-Jie Cai(蔡汉杰), Ping Lin(林平), Liang-Wen Chen(陈良文), Lei Yang(杨磊)
Chin. Phys. B, 2020, 29 (**4**): 048102. DOI: 10.1088/1674-1056/ab7807

Comparison study of GaN films grown on porous andplanar GaN templates

Shan Ding(丁姗), Yue-Wen Li(李悦文), Xiang-Qian Xiu(修向前), Xue-Mei Hua(华雪梅), Zi-Li Xie(谢自力), Tao Tao(陶涛), Peng Chen(陈鹏), Bin Liu(刘斌), Rong Zhang(张荣), You-Dou Zheng(郑有炓)
Chin. Phys. B, 2020, 29 (**3**): 038103. DOI: 10.1088/1674-1056/ab6c48

Density functional calculations of efficient H_2 separation from impurity gases (H_2, N_2, H_2O, CO, Cl_2, and CH_4) via bilayer g-C_3N_4 membrane

Yuan Guo(郭源), Chunmei Tang(唐春梅), Xinbo Wang(王鑫波), Cheng Wang(王成), Ling Fu(付玲)
Chin. Phys. B, 2019, 28 (**4**): 048102. DOI: 10.1088/1674-1056/28/4/048102

Influence of an inserted bar on the flow regimes in the hopper*

Yi Peng(彭毅)[1,2], Sheng Zhang(张晟)[1], Mengke Wang(王梦柯)[1,†], Guanghui Yang(杨光辉)[1], Jiangfeng Wan(万江锋)[3], Liangwen Chen(陈良文)[1], and Lei Yang(杨磊)[1]

[1] *Institute of Modern Physics, Chinese Academy of Sciences, Lanzhou* 730000, *China*
[2] *University of Chinese Academy of Sciences, Beijing* 100049, *China*
[3] *East China University of Technology, Nanchang* 330000, *China*

(Received 25 August 2020; revised manuscript received 23 October 2020; accepted manuscript online 1 December 2020)

We investigated the influence of an inserted bar on the hopper flow experimentally. Three geometrical parameters, size of upper outlet D_1, size of lower outlet D_0, and the height of bar H, are variables here. With varying H we found three regimes: one transition from clogging to a surface flow and another transition from a surface flow to a dense flow. For the dense flow, the flow rate follows Beverloo's law and there is a saturation of inclination of free surface θ. We plotted the velocity field and there is a uniform linear relation between the particle velocity and depth from the free surface. We also found that the required value of D_1 to guarantee the connectivity of flow is little smaller than D_0. For the transition from a surface flow to a dense flow, there is a jump of flow rate and the minimum θ for flowing is two degrees larger than the repose angle.

Keywords: hopper flow, inserted bar, flow type transition, free surface, velocity distribution

PACS: 81.05.Rm **DOI:** 10.1088/1674-1056/abcf40

1. Introduction

From industrial interests, granular materials discharging from hoppers have been widely studied.[1–8] Granular materials discharge constantly from a hopper under gravity, which is different from normal fluids[9,10] and the flow rate is independent of the hopper diameter D with some criterions satisfied.[3] To quantitively describe the flow rate, a widely accepted scaling formula called Beverloo's law was proposed by Beverloo *et al.* in 1961.[1] This formula has a unified form for various types of hoppers: $Q = C\rho_i\sqrt{gR}A$, where C is a dimensionless coefficient which depends on the material properties,[10,11] R is the equivalent hydrodynamic radius, ρ_i is the bulk density of the initial grain pack in the hopper, g is the acceleration of gravity, and A is the equivalent hydrodynamic section.[8]

According to the motion state, a steady hopper flow can be divided into four flow regions.[8] There is a bulk flow region except for near the bottom, where the particles move downward uniformly. Due to the existences of durative force chains, the granular temperature is low. If the inclination of the upper surface is larger than the inter-friction angle, this bulk flow region can be further divided into two sub-regions: mass flow region and avalanche flow region. At the end of the bulk flow region, there is a converging shear region with a dilation.[12] In this region there are shears between particles and the granular temperature is much higher than that in bulk flow region.[13] Consequently, particles are no more under shear and fall freely in the free falling region, where a few collisions occur.[14] The stagnant region appears in lower corners where the particles experience very slow creeping,[15] where the volume fraction is larger than those in other three regions. There is a sliding surface between the stagnant zone and converging shear region.[16]

To control the hopper flow, the effect of an insert has been studied for decades.[17–21] Zuriguel *et al.*'s experiment shows the presence of insert above the outlet reduces the probability of clogging.[22] The existence of insert will also result in the transition from funnel flow to mass flow. Moreover, it leads to the changes of flow rate and flow field. Under the insert, a free surface forms during the discharging, which was studied in Li *et al.*'s work.[23] The simulations showed that the free surface has a steady shape which could be fitted to be a paraboloid. Recently, Wojcik *et al.* performed a large scale experiment of hopper flow with inserts and found that the recommendations based on previous small scale studies are no longer a good solution in large scale tests.[24] As an obvious stagnant region exists in the hopper flow where the motions of particles are nearly static. One question is if there is a resemblance between this flow and the surface flow upon an erodible heap.[25,26] In this heap flow, it is found that the inclination angle depends on the flow rate and is influenced by sidewalls. There is a nearly linear profile of velocity along the flowing direction in flowing layers and the velocity decays exponentially in the heap.[27] This decay can be explained by the stress distribution being affected by the wall friction, that is, it has a potential correlation with Janssen effect.[28] In a new concept of dense granular-flow target, there also exists a free surface

*Project supported by the National Natural Science Foundation of China (Grant Nos. 11705256 and 11905272), National Postdoctoral Program for Innovative Talents, China (Grant No. BX201700258), and West Light Foundation of the Chinese Academy of Sciences (Grant No. 2018-98).

†Corresponding author. E-mail: wangmk@impcas.ac.cn

© 2021 Chinese Physical Society and IOP Publishing Ltd

under an inner tube.[29] The shape and velocity distribution are specially concerned because of the great influences on the capacity of heat remove.

Here we provide an experimental study of the free surface under an insert in the hopper. A long bar is inserted in an asymmetric hopper to present the details of the free surface. We study the influence of the bar on the flow rate, the shape of the surface, and the velocity field.

2. Methods

As shown in Fig. 1, the setup for experiments is a rectangular bin (200 cm×60 cm×6 cm). A bar, whose thickness is 3 cm, is inserted from the right side to create two chambers, that is, the upper chamber and the lower chamber. The distance between the lower surface of the bar and the bottom, H, can be adjusted in unit of 3 cm. The expanding distance can be adjusted and the height can be changed in 3 cm. The interval between the bar and walls is less than 3 mm. In the experiments, spherical plexiglass particles are used with the dispersity of diameter $d = 6 \pm 0.02$ mm. The outlet size is controlled by moving the bottom plate. In this study, there are three controlling parameters: D_0, D_1, and H. For simplicity, each case is denoted by D_1–D_0–H. For example, case 10–2–36 presents the case with $D_1 = 10$ cm, $D_0 = 2$ cm, and $H = 36$ cm. The weight of outflow is recorded by using an electronic balance with precision ± 0.1 g in a recording frequency 10 Hz. When the flow is steady, a time-averaged flow rate is obtained by linear fitting of the cumulative weight. To against the electrostatics, anti-static spray is used and the humidity is controlled to be 45% during the experiments.

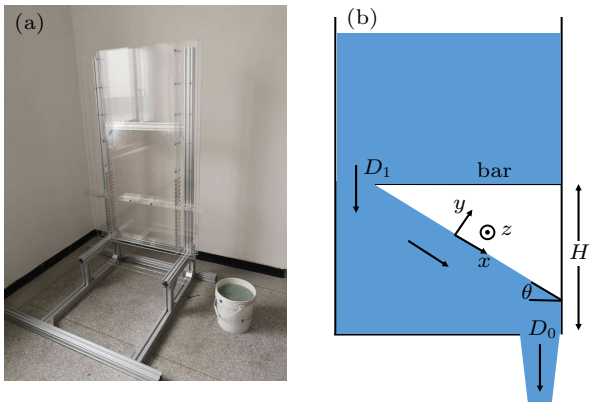


Fig. 1. (a) The equipment in this study. (b) A schematics of a dense flow (see the definition in text) with an asymmetric bar. The coordinate frame is plotted.

A fast-industrial camera (Revealer 2F04) is employed to shoot the discharging process. The shooting area is around 500 mm×400 mm and the image resolution is 2240 × 1640. The velocity measurement of the particles close to the sidewall is based on their moving tracks. With visible diameter of the particle in the picture frame of video, the position of the particle can be recognized successfully. If the same particle can be tracked within subsequent frames, the velocity vector of the particle is obtained. In the calculation, we also consider different corrections, such as the distortion of the lens system and rotation of the camera to the ground. In the surface of rapid flows, the particles in this region move faster, so a high 800 frames per second (FPS) resolution is adopted for tracking. Here we use the CSRT algorithm (built-in function in OpenCV) for particle tracking. This algorithm called CSRDCF++ (discriminative correlation filter with channel and spatial reliability) is the best performing real-time tracker in the Visual Object Tracking VOT2017 challenge.[30]

3. Results and discussion

In the beginning, the lower chamber is filled and the up chamber is loaded with 400 mm-high particles. After the opening of lower outlet D_0, according to the variation of instantaneous flow rate with time, the flowing process can be divided into two stages. The first stage is for the partial drainage of the lower chamber and the formation of an inclined free surface. In this stage, there is an obvious fluctuation of the flow rate. The second stage is for the stable flow that the particles in the upper chamber flow into the lower chamber continuously. As shown in Fig. 2, with small H, finally there is a clogging after stage one. The slope, which could be seen as a repose angle θ_r here, is $\sim 19.5^\circ$. As H increases, a surface flow appears which is defined by the observation that the space of the lower outlet is not full of particles. This means, there is no interaction between the jet and right sidewall. It is natural to deduce that in this surface flow regime, the flow rate does not depend on the lower outlet size D_0. This flow rate saturates when H exceeds 30 cm. Then the flow above the lower outlet becomes dense and the surface in the lower chamber can be presented as an incline.

In the dense flow regime, we can also confirm the Beverloo scaling law $Q \sim (D_0 - kd)^\alpha$ by varying outlet size D_0 (see Fig. 3). Accordingly, the hopper is quasi-two-dimensional. The fitting power $\alpha = 3/2$ and coefficient of 'empty annulus' $k = 0.5$. This result shows that the scaling law is not broken by inducing an obstacle.[31,32] The empty annulus here is only one half of the particle diameter, which is consistent with the original assumption adopted by Brown and Richards.[33] However, this value is smaller than the usual value of three-dimensional hopper flow[3] and also smaller than the value in previous simulations of the quasi-two-dimensional hopper flow.[31] It is worth noted that there is still a stable dense flow with $D_0 = 1.3$ cm, which is just 2.1 times of the particle diameter, and correspondingly the flow rate is 78.3 g/s.

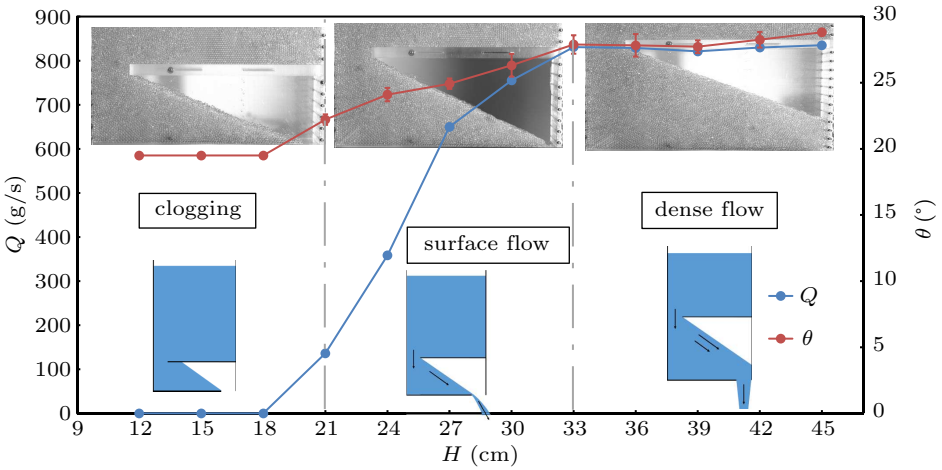


Fig. 2. Variations of flow rate and inclination of surface by varying H. Three flow regimes (clogging, surface flow, and dense flow) are recognized. $D_1 = 10$ cm and $D_0 = 4$ cm are adopted.

The formation of the surface is shot by a camera during the flow and analyzed by a visualization code (see Section 2). It shows that in both surface flow and dense flow regimes, the variation of the surface over time is small and the surface can be presented as a simple slope. In the surface flow regime, the inclination decreases to 22° when H decreases to 21 cm. In the dense flow regime, where the outlet size D_0 is fixed at 4 cm, the inclination of the slope is 27.8° and seems to be invariable with changing H. If we fixed H and changed the outlet size D_0, the inclination increases from 23.8° to 29.2° when D_0 increases from 1 cm to 5 cm (Fig. 3). It also indicates that the inclination is unchanged when $D_0 \geq 5$ cm, regardless of the continued increase of the flow rate.

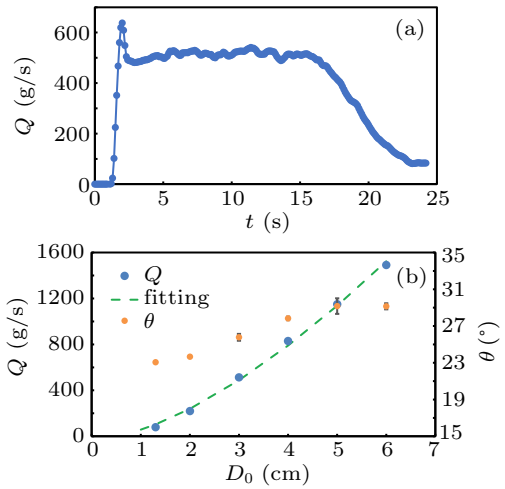


Fig. 3. (a) Profile of Q with time t where $D_0 = 3$ cm, $D_1 = 10$ cm, and $H = 36$ cm. (b) Variation of flow rate and inclination in dense flow regime by varying lower outlet size D_0. $H = 36$ cm and $D_1 = 10$ cm are adopted.

To conveniently analyze the distribution of velocity under the surface, for each case, the x coordination is set to be parallel to the surface and the y coordination is set to be perpendicular to the surface (see Fig. 1(b)). At the surface, the value of y-coordinate is zero. Here the velocity distribution of particles close to the wall is analyzed by neglecting the difference in z direction.[26,34] Former studies showed that in heap flow, the velocity distribution with depth can be divided into two parts: a linear dependence region changing to an exponential decay region.[26,35] Here the similar profile is reproduced in both the surface flow and dense flow regimes (see surface flow case 10–4–21 and dense flow case 10–2–36). Following the former work, here the depth of the flow, h, is defined as the linear part intersecting the x axis. In Ref. [36], the authors obtained a scaling relation in heap flow at low flow rate limit: $h \sim Q^{2/7}$. From Fig. 4(a), it is noticed that in the dense flow, the slope of the linearity is nearly the same (~ 0.08) except case 10–2–36. If the flow rate can be roughly evaluated as $Q = \int_{-h}^{0} \phi v_x W \, \mathrm{d}y$, where W is the channel width, by using the uniform linear relation between v_x and y, we will derive a quadratic relation between Q and h: $Q \sim h^2$, which is also demonstrated in Fig. 4(b).

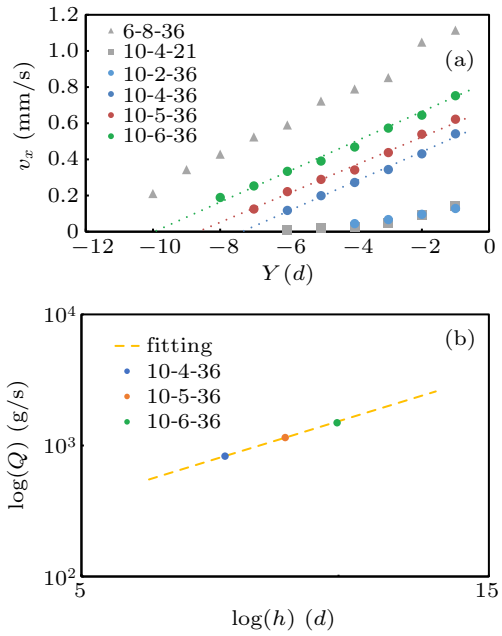


Fig. 4. (a) Profiles of velocity v_x with depth from the surface. Triangles denote the heap flow. Dotted lines are for visual guide. (b) Scaling relation between Q and h.

For the existence of an inserted bar, one interesting issue is whether the connectivity of the dense flow between upper and lower chambers will be affected by the bar. It is trivial to know that this connectivity will be blocked if $D_1 < 1d$, leading to a clogging. Here we set $D_0 = 4$ cm and measure the variation of the flow rate with decreasing D_1. The results show that the flow rate is affected if $D_1 < 3.5$ cm, leading to an obvious reduction of the flow rate (see Fig. 5). It is quite surprising that this critical value of D_1 is even smaller than the fixed value of D_0, which is confirmed in the additional cases with $D_0 = 6$ cm. A potential explanation is that for the flow across D_1, there is no 'empty annulus'.

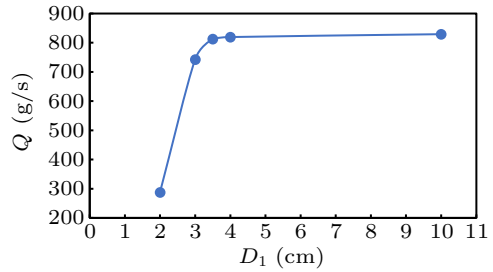


Fig. 5. Variation of flow rate in dense flow regime by varying upper outlet size D_1. $H = 36$ cm and $D_0 = 4$ cm are adopted.

Another question is whether there is a jump of flow rate for the transition from clogging to surface flow. For this equipment, owing to the fact that H can be only adjusted in unit of 3 cm, we can drive the system towards the clogging state by increasing D_1 to let the aspect ratio $H/(D-D_1-D_0)$ approach to $\tan\theta_r$. According to the clogging transition happening between $H = 18$ cm to $H = 30$ cm, here we fix $H = 21$ cm and $D_0 = 4$ cm and find that there is a clogging when $D_1 \leq 3.5$ cm (see Fig. 6). Thus the critical aspect ratio $H/(D-D_1-D_0) = 21/52.5 = 0.4$ which provides the corresponding angle of 21.8° and the minimum flow rate in this system is 18.2 g/s with $D_1 = 3.6$ cm. This angle is 2° larger than the repose angle θ_r in the clogging flow, which is attributable to dilatancy[37,38] and is often the angle of metastable state in previous reports.[39,40] Additionally, there is a roughly linear dependence of D_1 on the flow rate, so is the inclination of the surface. These results suggest the influences of fore and rear boards, which are similar in the heap flow (see below).

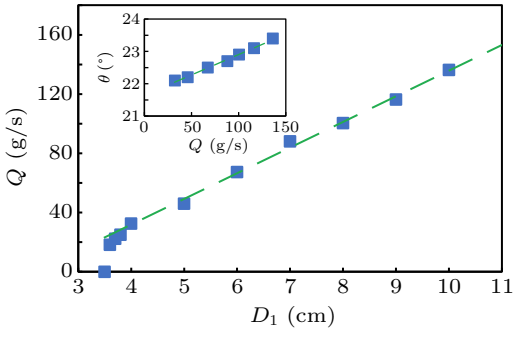


Fig. 6. Variation of flow rate in surface flow regime by varying upper outlet size D_1. $H = 21$ cm and $D_0 = 4$ cm are adopted. Dotted line is for visual guide. Insert: variations of inclination of surface.

In previous study of heap flow,[26] the authors showed that with considering the influence from sidewalls, there is a linear relationship between the input flow rate and critical inclination. A force balance leads to $\tan\theta = \mu_i + \frac{h}{W}\mu_w$, where μ_i is a constant internal friction coefficient, μ_w is an effective friction coefficient accounting for both sliding and rolling of the grains on the walls, W is the channel width, and h is the height of the flowing layer. To verify this conclusion that there is a linear relationship between the input flow rate and critical inclination in our experiment, for initialization the upper outlet D_1 is closed and the upper chamber is filled. H is set to be large enough to guarantee that after the opening of D_1, the flow at D_1 is dilute and the particles in the upper chamber fall freely on the heap. The relationship between the flow rate and D_1 also obeys Beverloo's law and the parameters are the same as those in Fig. 3 (not shown here). From Fig. 7, there are similar results to Ref. [26]. However, due to an obvious diverge between the function value of θ or $\tan\theta$ until $\theta > 45°$ while the corresponding flow rate is too large, it is hard to judge whether θ or $\tan\theta$ depends on the flow rate linearly. We do a linear fitting between θ and the flow rate to obtain an intercept on the y axis, which is 21.7° and this angle is consistent with the critical value in the surface flow. Compared with the conditions in Refs. [26,41], these results confirm that the dependence of the flow rate on the inclination is uniform in both heap flow and surface flow and is not affected by changing the materials or the roughness of the bottom. In contrast, figure 3 shows that in the dense flow regime, there is a saturation of inclination with increasing flow rate. This disagreement needs further investigation.

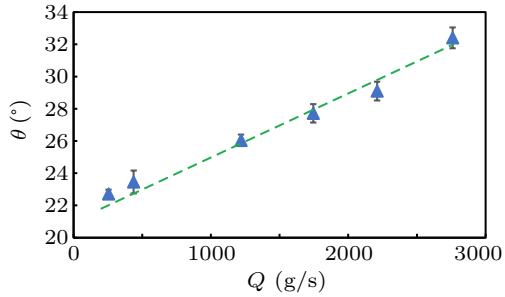


Fig. 7. Inclination of free surface vs. flow rate in heap flow. $H = 36$ cm and $D_0 = 8$ cm are adopted. Dotted line is for visual guide.

4. Conclusion

We investigated the influence of a bar on a granular flow in a rectangular bin experimentally. We found the varying of the height of the bar results in the transitions from clogging to a dense flow via a surface flow regime. Below the bar, the free surface of flow can be described as a slope. It seems that the change of the flow rate from clogging to surface flow is a jump and the minimum flow rate is 18.2 g/s. The slope of surface for this jump is larger than the tangent of repose angle. In the dense flow regime, the Beverloo scaling law will remain

valid with the introduction of the bar. The slope of surface will saturate with increasing flow rate. The velocity distribution was analyzed and is consistent with that in a heap flow. To ensure the connectivity of the flow, the allowable distance between the bar and sidewall can be slightly smaller than the outlet size. Finally, we produced a heap flow in this bin and found a linear dependence of the flow rate on the slope of surface.

References

[1] Beverloo W A, H A Leniger and van de Velde J 1961 *Chemical Engineering Science* **15** 260
[2] Brown R L 1961 *Nature* **191** 458
[3] Nedderman R, Tuzun U, Savage S and Houlsby G 1982 *Chemical Engineering Science* **37** 1597
[4] Hirshfeld D, Radzyner Y and Rapaport D C 1997 *Phys. Rev. E* **56** 4404
[5] Mankoc C, Janda A, Arévalo R, Pastor J, Zuriguel M, Garcimartín I and Maza D 2008 *Granular Matter* **10** 469
[6] Hilton J E and Cleary P W 2011 *Phys. Rev. E* **84** 011307
[7] Janda A, Zuriguel I and Maza D 2012 *Phys. Rev. Lett.* **108** 248001
[8] Saleh K, Golshan S and Zarghami R 2018 *Chemical Engineering Science* **192** 1011
[9] Bertho Y, Giorgiutti-Dauphine F and Hulin J P 2003 *Phys. Rev. Lett.* **90** 144301
[10] Anand A, Curtis J S, Wassgren C R, Hancock B C and Ketterhagen W R 2008 *Chemical Engineering Science* **63** 5821
[11] Zhang S, Lin P, Wang C L, Tian Y, Wan J F and Yang L 2014 *Granular Matter* **16** 857
[12] Vidyapati V and Subramaniam S 2013 *Industrial & Engineering Chemistry Research* **52** 13171
[13] Rubio-Largo S M, Janda A, Maza D, Zuriguel I and Hidalgo R C 2015 *Phys. Rev. Lett.* **114** 238002
[14] Lin P, Zhang S, Qi J, Xing Y M and Yang L 2015 *Physica A* **417** 29
[15] Tuzun U and R M Nedderman 1982 *Powder Technology* **31** 27
[16] Babout L, Grudzien K, Maire E and Withers P J 2013 *Chemical Engineering Science* **97** 210
[17] Johanson J R 1968 *Powder Technology* **1** 328
[18] Tuzun U and Nedderman R M 1985 *Chemical Engineering Science* **40** 325
[19] Yang S C and Hsiau S S 2001 *Powder Technology* **120** 244
[20] Johanson K 2006 *Powder Technology* **170** 109
[21] Endo K, Reddy K A and Katsuragi H 2017 *Phys. Rev. Fluids* **2** 094302
[22] Zuriguel I, Janda A, Garcimartin A, Lozano C, Arevalo R and Maza D 2011 *Phys. Rev. Lett.* **107** 278001
[23] Li X D, Wang J F, Zhang S, Lin P and Yang L 2017 *PloS One* **12** e0187435
[24] Wojcik M, Tejchman J and Enstad G G 2012 *Powder Technology* **222** 15
[25] Delannay R, Louge M, Richard P, Taberlet N and Valance A 2007 *Nat. Mater.* **6** 99
[26] Taberlet N, Richard P, Valance A, Losert W, Pasini José Miguel, Jenkins J T and Delannay R 2003 *Phys. Rev. Lett.* **91** 264
[27] Bi W, Delannay R, Richard P, Taberlet N and Valance A 2005 *J. Phys.: Condens. Matter* **17** S2457
[28] Martínez E, González-Lezcano A, Batista-Leyva A J and Altshuler E 2016 *Phys. Rev. E* **93** 062906
[29] Yang L and Zhan W L 2015 *Science China-Technological Sciences* **58** 1705
[30] Kristan M, Ales Leonardis, Matas J, Felsberg M and Pflugfelder R 2018 *IEEE International Conference on Computer Vision Workshops*
[31] Yang G H, Zhang S, Lin P, Tian Y, Wan J and Yang L 2016 *Granular Matter* **18** 1
[32] Wan J F, Zhang S, Tian Y and Lin P 2016 *Journal of Nuclear Science and Technology* **53** 1809
[33] Brown R L and Richards J C 1965 *Rheologica Acta* **4** 153
[34] Zhang S, Yang G, Lin P, Chen L and Yang L 2019 *Euro. Phys. J. E* **42** 14
[35] Orpe A V and Khakhar D V 2007 *Journal of Fluid Mechanics* **571** 1
[36] Jop P, Forterre Y and Pouliquen O 2005 *Journal of Fluid Mechanics* **541** 167
[37] Pouliquen O and Renaut N 1996 *Journal De Physique Ii* **6** 923
[38] Marteau E and Andrade J E 2018 *Acta Geotechnica* **13** 549
[39] Nagel S 1992 *Rev. Mod. Phys.* **64** 321
[40] Zheng P 2011 *Acta Phys. Sin.* **60** 680 (in Chinese)
[41] Taberlet N, Richard P, Henry E and Delannay R 2004 *Europhys. Lett.* **68** 515